Science Advances

AAAS

advances.sciencemag.org/cgi/content/full/2/7/e1601001/DC1

Supplementary Materials for

Early scattering of the solar protoplanetary disk recorded in meteoritic chondrules

Yves Marrocchi, Marc Chaussidon, Laurette Piani, Guy Libourel

Published 1 July 2016, *Sci. Adv.* **2**, e1601001 (2016)
DOI: 10.1126/sciadv.1601001

This PDF file includes:

Supplementary Materials

O-isotope mass balance calculation

The initial idea of the present calculation is based on experimental studies that have revealed that varying amounts of oxygen can be dissolved in FeS melts as a function of fO_2 (*12*). In addition, at fO_2 higher than the Iron-Wüstite buffer (IW) the molar fraction of O within FeS melts approaches the magnetite side of the sulfide-magnetite join, producing O-rich Fe-S-O melts. Hence, Fe-S-O melts with varying S/O ratio can be generated at magmatic temperatures (i.e., > 930°C), leading to the crystallization of sulfide-magnetite associations in varying proportions that bear striking resemblances to those observed within CV chondrules. Hence, our petrographic observations strongly suggest that chondrule magnetites could result from the crystallization of high temperature magmatic FeSO melts generated by gas-melt interactions during the chondrule-forming event(s).

Here, we consider as an end-member model that low-Ca pyroxene precipitates instantaneously from the melt when it is saturated, as has been suggested in experiments (*43*). In addition, FeS are mainly present within the low-Ca pyroxene outer rim and their amount increases with the abundance of low-Ca pyroxene within chondrules (*10*). FeS formation obeys complex high-temperature processes of sulfur solubility within chondrule melts, followed by sulfide saturation (*10*). Hence, the evolution of chondrule melts towards more silicic compositions *via* gas-melt interactions (from PO to PP) induces the immiscibility of FeS melts at much lower S contents, leading to co-crystallization of iron sulfides and low-Ca pyroxenes (*10*). We consider, similarly to the formation of pyroxene, that FeS forms instantaneously when chondrule melt reaches sulfide saturation, the ratio between FeS and SAM being controlled by the fO_2. Hence, the formation of pyroxenes, FeS and magnetite in a given chondrule can summarized by the following reactions

$$f(Mg_2SiO_4)_{ol} + (1-f)Fe_{metal} + fSiO_{2(melt)} + \frac{(1-f)}{2}\left[xS_{2(gas)} + (1-x)O_{2(gas)}\right] =$$

$$2f(MgSiO_3)_{opx} + (1-f)\left[xFeS_{sulf} + (1-x)FeSO_{SAM}\right] \quad \text{(S1)}$$

$$SiO_{(gas)} + {}^{1}/_{2}\, O_{2(gas)} = SiO_{2(melt)} \quad \text{(S2)}$$

where *f* is the modal abundance of olivine relative to Fe metal and x is the modal abundance of sulfide relative to magnetite in a given chondrule.

Crystallization of FeSO melts would induce the formation of FeS and SAM, as revealed by laboratory experiments (*12*). Following the approach used to describe the variation of oxygen isotopic composition of pyroxene formed by interaction of type I chondrule melts with a SiO_2-rich gas (*21*, *22*), oxygen isotopic mass balance for equation S1 can be written as (similar form for $\delta^{17}O$ or $\delta^{18}O$)

$$N \times \delta^{17,18}O_{bulk} = 6f \times \delta^{17,18}O_{opx} + (1-f) \times (1-x) \times \delta^{17,18}O_{SAM} = 4f \times$$

$$\delta^{17,18}O_{ol} + 2f \times \delta^{17,18}O_{SiO_2(melt)} + (1-f)(1-x) \times \delta^{17,18}O_{gas} \quad \text{(S3)}$$

with

$$N = 6f + (1-f) \times (1-f) \quad \text{(S4)}$$

This mass balance can be rewritten by taking into account $\Delta^{18}O_{SAM\text{-}opx}$, which corresponds to the equilibrium oxygen isotopic fractionation between immiscible magnetite and orthopyroxene (or between immiscible magnetite and melt assuming no significant isotopic fractionation between melt and orthopyroxene, $\Delta^{18}O_{SAM\text{-}opx} = \delta^{18}O_{SAM} - \delta^{18}O_{opx} = -3$ ‰, according to (*44*)), as

$$\delta^{17,18}O_{bulk} = \delta^{17,18}O_{SAM}\left(\frac{6f}{N} + \frac{(1-f)(1-x)}{N}\right) - \frac{6f}{N}\,\Delta^{17,18}O_{SAM-opx} \quad \text{(S5)}$$

We consider as a first approximation that in Eqn. S2 there is no significant O isotopic fractionation between O incorporated in the melt and O in the gas so that

$$\delta^{17,18}O_{SiO_2(melt)} = \delta^{17,18}O_{gas} \quad \text{(S6)}$$

Hence, Eqn. S3 can be rewritten as

$$\delta^{17,18}O_{bulk} = \frac{6f}{N}\,\delta^{17,18}O_{opx} + \frac{(1-f)(1-x)}{N}\,\delta^{17,18}O_{SAM} = \frac{4f}{N}\,\delta^{17,18}O_{ol} + \delta^{17,18}O_{gas}\left[\frac{2f}{N} + \frac{(1-f)(1-x)}{N}\right] \quad \text{(S7)}$$

Combining Eqns. (S5) and (S7), the gas with which a given chondrule equilibrated has an oxygen isotopic ratio given by

$$\delta^{17,18}O_{gas} = \frac{\delta^{17,18}O_{SAM}\left(6f+(1-f)(1-x)\right) - 6f\Delta^{17,18}O_{SAM-opx} - 4f\delta^{17,18}O_{ol}}{2f+(1-f)(1-x)} \quad \text{(S8)}$$

By simplification, we attain an equation allowing the O-isotopic composition of the gas to be calculated as a function of $\delta^{18}O_{ol}$, $\delta^{18}O_{SAM}$, f and x

$$\delta^{17,18}O_{gas} = \delta^{17,18}O_{SAM} - \frac{2f\left(3\Delta^{17,18}O_{SAM-opx} + 2\delta^{17,18}O_{ol} - 2\delta^{17,18}O_{SAM}\right)}{(1+f)+x(f-1)} \quad \text{(S9)}$$

$\delta^{18}O_{ol}$ and $\delta^{18}O_{SAM}$ correspond to the measured oxygen isotope composition for olivine and magnetite in a given chondrule. It should be noted that the variability of $\delta^{18}O_{ol}$ and $\delta^{18}O_{SAM}$ measured in a given chondrule was taken into account in the calculations and corresponds to the error bars reported in Fig. 3. All calculations were performed with an olivine modal abundance of 0.9 relative to metal (0.1). All SAM-bearing chondrules show a FeS modal abundance of FeS of ≈ 0.8 relative to magnetite (0.2). However, it should be noted that the modal abundances of olivine relative to metal and of FeS relative to magnetite have little influence on the calculation, with the more sensitive parameters being $\delta^{18}O_{ol}$ and $\delta^{18}O_{SAM}$.

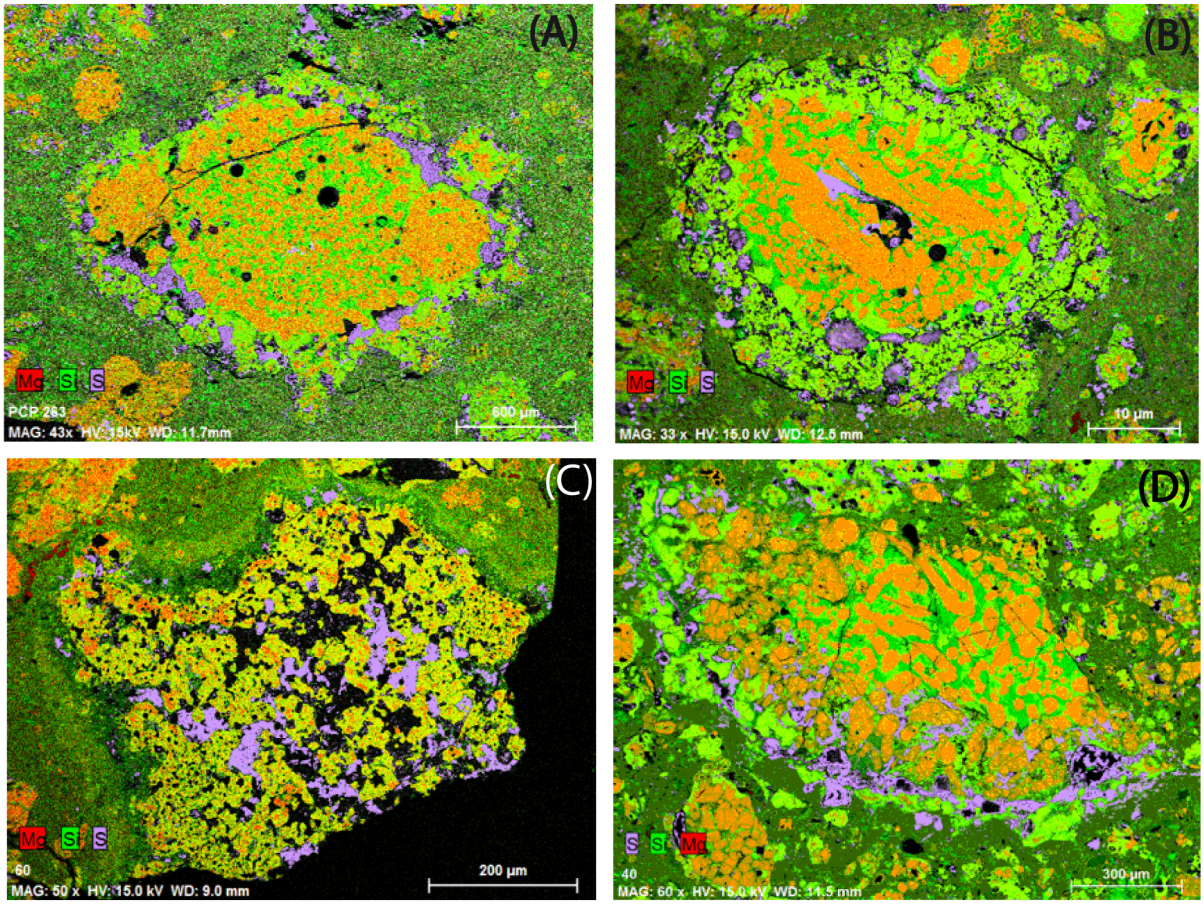

fig. S1. Compiled EDX maps of Si, Mg, and S of four chondrules, revealing the mineralogy of the different phases: olivine (orange), low-Ca pyroxene (pale green), glassy mesostasis (dark green) and sulfides (purple). The black areas associated with sulfides correspond to magnetite. These maps show that sulfides and SAMs are mainly associated with low-Ca pyroxenes in the outer zone of chondrules. (**A**) Kaba Ch-3. (**B**) Kaba Ch-7. (**C**) Kaba Ch-12. (D) Vigarano Ch-52.

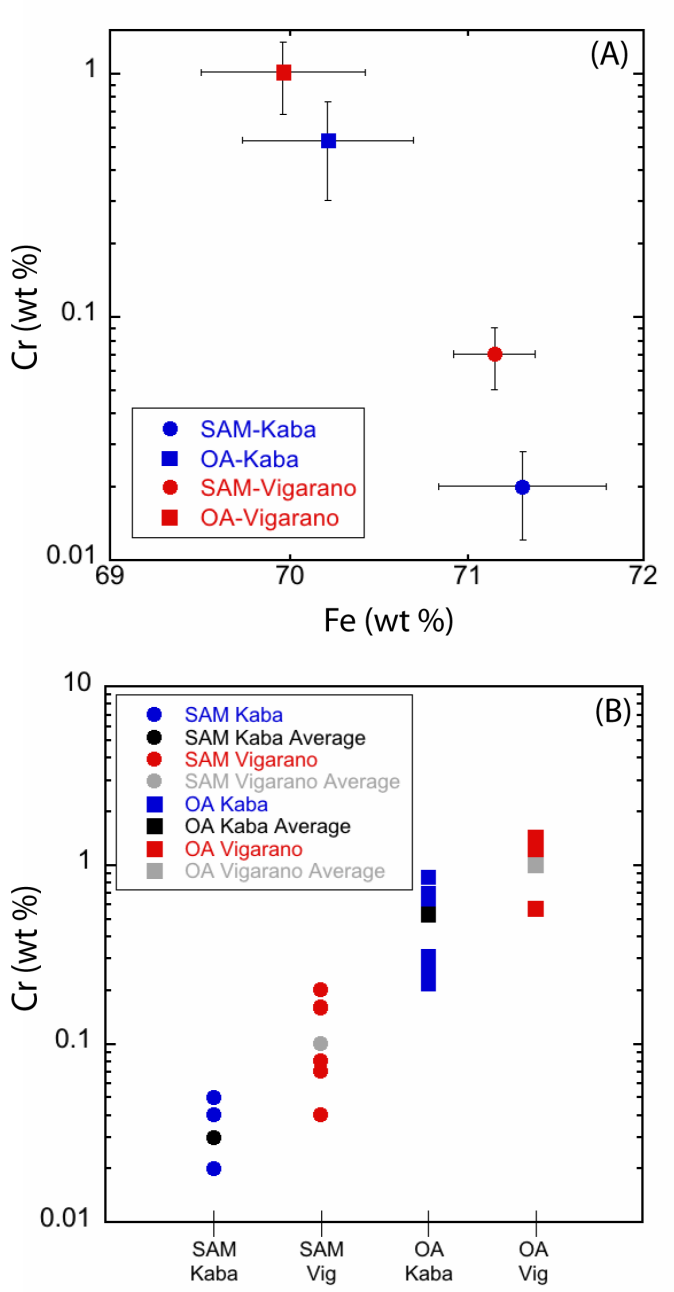

fig. S2. (**A**) Average chromium versus average iron content (wt%) of SAM and magnetite-bearing OA in the Kaba and Vigarano CV3 chondrites. (**B**) Chromium content (wt%) of SAM and magnetite-bearing OA in the Kaba and Vigarano CV3 chondrites. Magnetites within OAs are Cr-rich whereas SAM are characterized by a low Cr content, revealing the absence of a genetic relationship between these two textures.

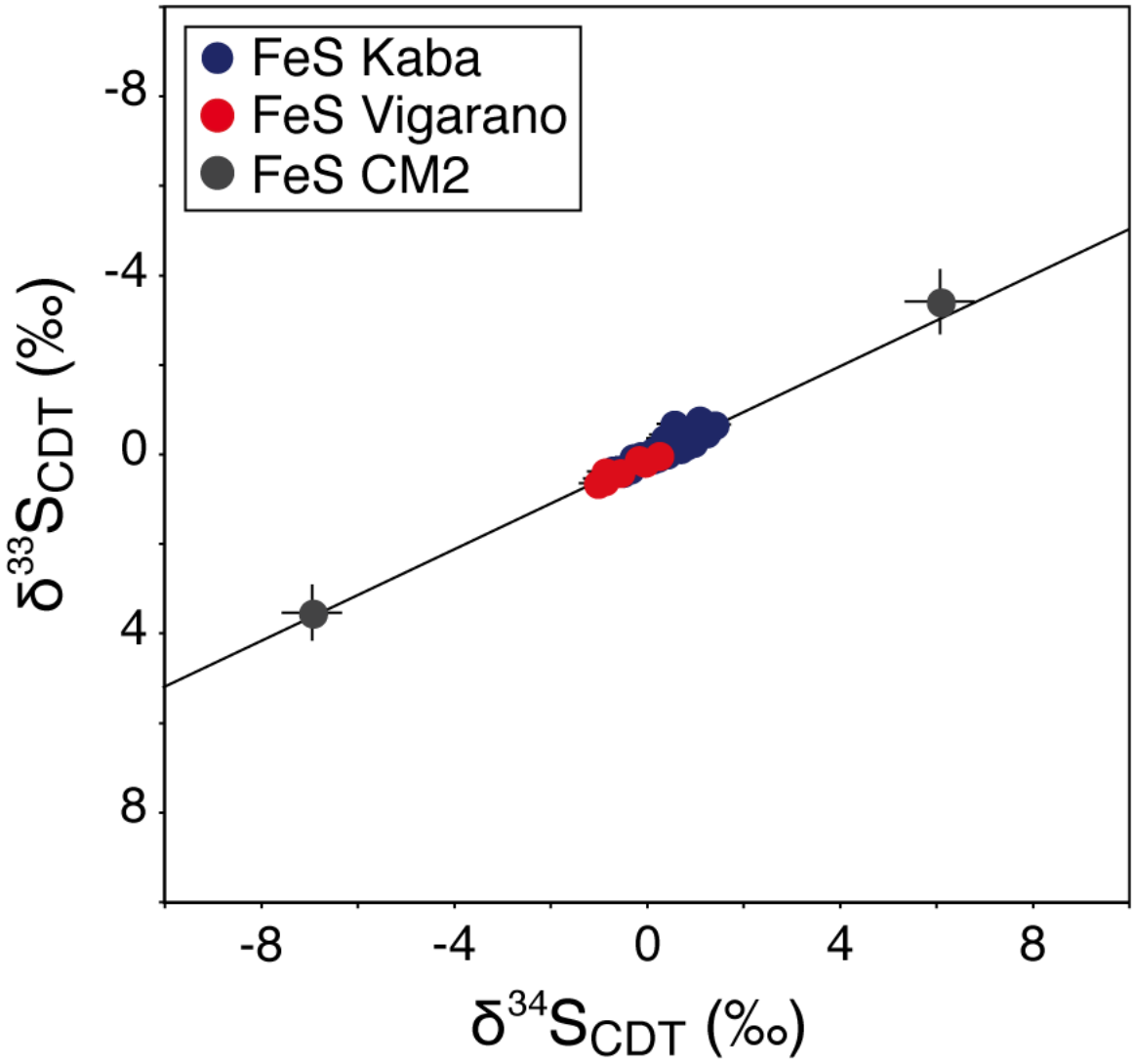

fig. S3. Sulfur isotopic composition of troilite grains present in SAM within chondrules of the Kaba and Vigarano CV3 chondrites. All data plots on the Terrestrial Fractionation Line (TFL), within a narrow range of variation centered on 0 ‰. The sulfur isotopic variability observed in FeS from aqueously altered CM chondrites are shown for comparison.

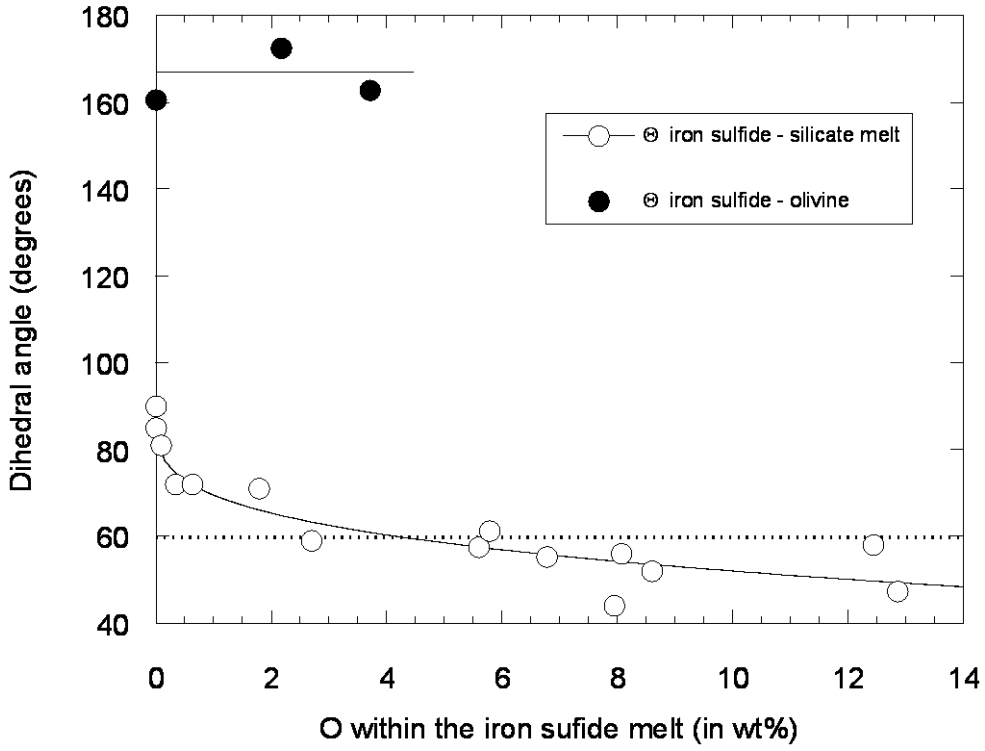

fig. S4. Influence of the amount of oxygen dissolved in FeS melts on silicate mineral/Fe-S-O mattes dihedral angles. Two distinct behaviors can be observed. In the absence of silicate melts, the amount of O dissolved in FeS melts has a critical effect on silicate minerals/FeSO mattes dihedral angles, with the transition from non-wetting to wetting behavior occurring at an O concentration around 4 wt% (fig. S4). Conversely, Fe-S-O mattes in contact with silicate melts behave as non-wetting liquids regardless of their oxygen content.

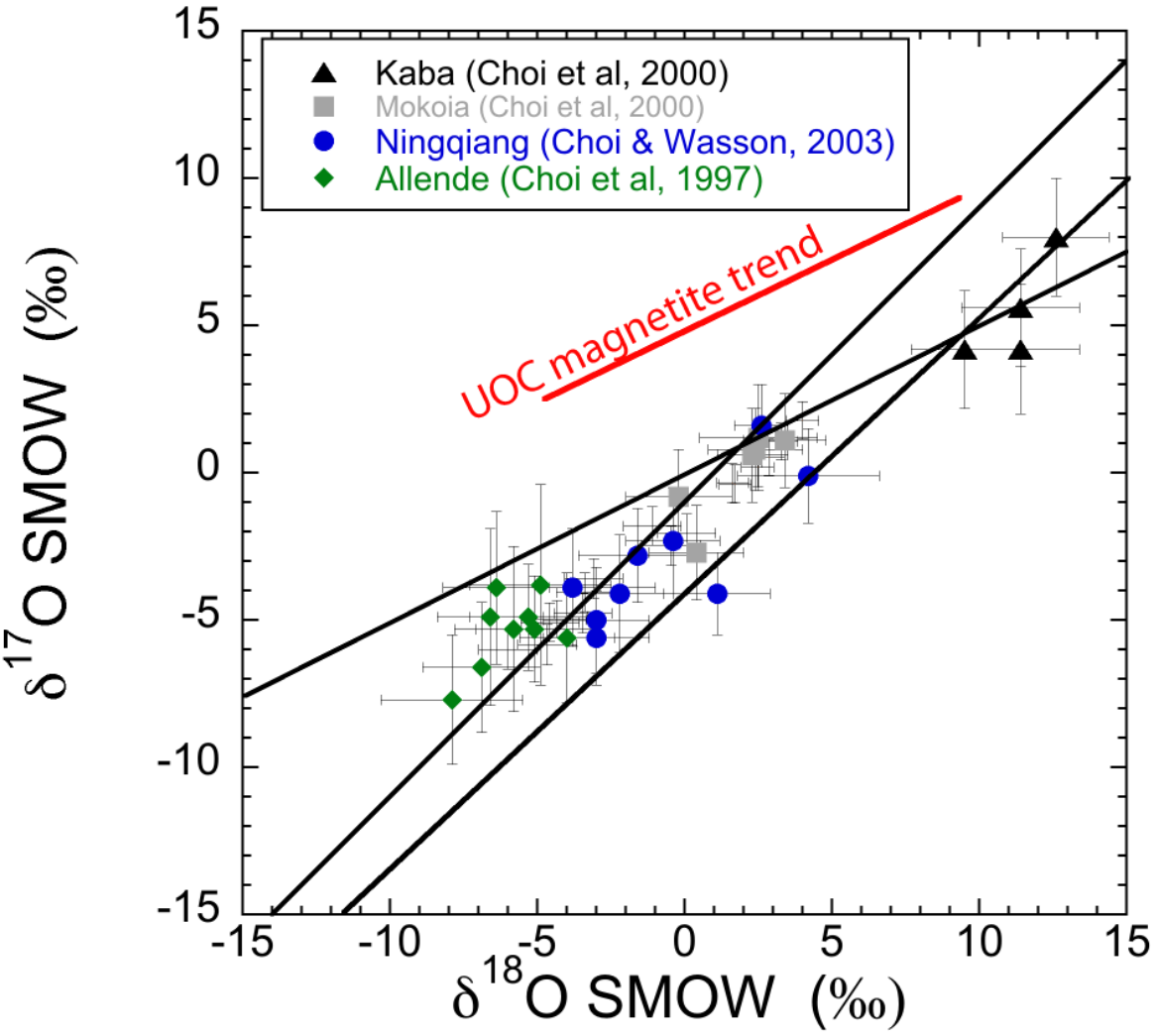

fig. S5. Three-oxygen isotope diagram showing previous results of oxygen isotopic compositions of magnetites in CV chondrules (*16, 45*). These results show that magnetites in CV chondrules do not follow a mass-dependent relationship, contrasting with magnetites in chondrules from unequilibrated ordinary chondrites (UOC, red line). The latter suggests formation via aqueous alteration, whereas the mass-independent signature of magnetites in CV chondrules clearly indicates a high temperature origin, in good agreement with the data reported in this study.

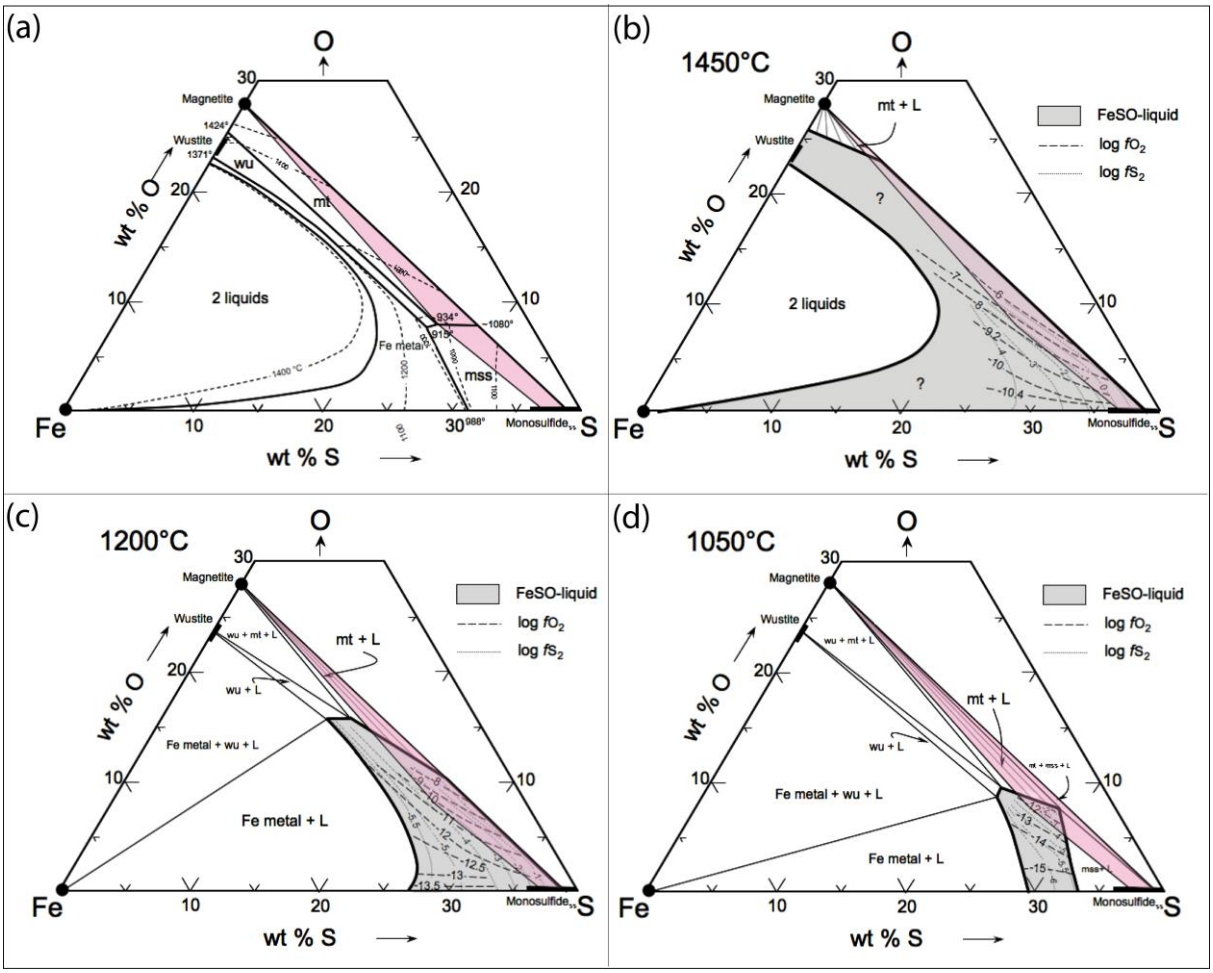

fig S6. (**a**) Liquidus relation in a portion of the FeSO system. The pink triangle corresponds to the portion of the phase diagram possible for chondrule formation according to the absence of wüstite within chondrules. (**b**) Relationship between fS_2 and fO_2 in a portion of the FeSO system at 1450°C and 1 atm total pressure. The sulfide-magnetite field (pink triangle) suggests the formation of FeS-Fe_3O_4 associations at fO_2 several order of magnitude higher than the IW buffer. (**c**) Relationship between fS_2 and fO_2 in a portion of the Fe-S-O system at 1200°C and 1 atm total pressure. (**d**) Relationship between fS_2 and fO_2 in a portion of the Fe-S-O system at 1050°C and 1 atm total pressure (*46*).

			O	Mg	Al	Cr	Fe	Si	P	Ca	Ni	Total (wt%)
Kaba	Ch-3	SAM	26.49	0.15	bdl	0.03	71.77	0.18	bdl	bdl	0.02	98.64
		SAM	27.12	0.33	bdl	bdl	71.53	0.30	bdl	bdl	bdl	99.28
		SAM	27.44	0.35	bdl	0.04	71.14	0.27	bdl	bdl	bdl	99.23
		SAM	27.31	0.21	bdl	0.05	71.05	0.59	bdl	bdl	bdl	99.22
		SAM	26.49	0.41	bdl	bdl	70.75	0.31	bdl	bdl	0.02	97.98
		SAM	27.10	0.17	bdl	0.03	72.00	0.07	bdl	bdl	0.04	99.41
		SAM	26.60	0.27	bdl	0.04	71.03	0.18	bdl	bdl	0.03	98.15
		SAM	26.58	0.19	bdl	bdl	71.55	0.08	bdl	bdl	0.04	98.45
		SAM	26.69	0.36	bdl	bdl	71.42	0.12	bdl	0.04	0.05	98.68
		SAM	27.10	0.20	bdl	bdl	70.90	0.95	bdl	bdl	bdl	99.14
		OA	27.99	0.08	bdl	0.28	70.53	0.04	bdl	0.03	0.08	99.03
		OA	26.38	0.07	bdl	0.60	70.72	0.09	0.03	0.05	0.40	98.34
Kaba	Ch-7	OA	26.60	0.27	bdl	0.69	70.20	0.01	bdl	0.04	0.06	97.87
		OA	27.33	0.14	bdl	0.52	70.89	0.02	0.03	0.05	0.49	99.46
		SAM	26.32	0.13	bdl	0.05	70.89	0.05	bdl	0.05	0.27	97.77
		OA	26.93	0.14	bdl	0.26	69.82	0.06	0.03	0.05	2.92	100.21
		OA	26.67	0.21	bdl	0.65	69.90	0.03	0.04	bdl	0.73	98.23
		OA	26.16	0.15	bdl	0.56	70.09	0.02	0.05	bdl	1.71	98.74
		SAM	26.79	0.10	bdl	bdl	70.26	0.81	bdl	0.20	0.15	98.30
		SAM	26.92	0.10	bdl	bdl	71.23	0.01	bdl	bdl	0.22	98.49
		OA	27.80	0.06	bdl	0.31	70.65	0.20	0.07	bdl	bdl	99.09
Kaba	Ch-12	OA	27.96	0.04	bdl	0.22	70.41	0.07	0.03	bdl	0.07	98.81
		SAM	27.02	0.07	bdl	0.04	72.03	0.01	bdl	bdl	0.09	99.25
		SAM	26.42	0.07	bdl	bdl	71.90	0.01	bdl	bdl	0.05	98.45
		SAM	26.52	0.11	bdl	0.02	71.51	0.13	bdl	bdl	bdl	98.29
		SAM	27.65	0.16	bdl	0.02	71.26	0.10	bdl	bdl	0.02	99.20
		OA	27.57	0.53	0.11	0.86	69.83	0.03	0.58	0.24	bdl	99.75
		OA	27.09	0.57	0.10	0.86	69.29	0.03	0.56	0.19	0.02	98.72
Vigarano	Ch-52	SAM	27.74	0.16	0.35	0.07	71.42	0.01	bdl	bdl	bdl	99.74
		SAM	27.73	0.16	0.36	0.08	71.21	0.01	bdl	bdl	bdl	99.56
		SAM	27.67	0.16	0.53	0.04	70.83	0.01	bdl	bdl	bdl	99.24
		SAM	27.12	0.14	0.52	0.04	71.05	0.01	bdl	bdl	bdl	98.88
		SAM	27.06	0.17	0.58	0.09	70.98	0.01	bdl	bdl	bdl	98.89
		SAM	27.23	0.14	0.43	0.08	71.38	0.02	bdl	bdl	bdl	99.30
		OA	27.21	0.19	0.68	1.21	69.53	0.01	bdl	bdl	bdl	98.84
		OA	27.26	0.22	0.51	1.43	69.12	0.01	bdl	0.03	0.07	98.65
		OA	27.26	0.15	0.63	0.57	70.38	0.19	0.04	0.05	0.12	99.38
		OA	27.09	0.16	0.59	1.09	70.10	0.01	0.02	0.03	0.07	99.16
		OA	27.03	0.13	0.68	0.57	70.27	0.02	bdl	bdl	bdl	98.70
		OA	27.26	0.10	0.27	1.17	70.18	0.01	bdl	bdl	0.05	99.04
		OA	27.55	0.09	0.40	1.04	70.16	0.00	bdl	bdl	bdl	99.24

table S1. Chemical composition of magnetites in four different chondrules from Kaba and Vigarano. SAM = Sulfide-associated magnetites. OA = opaque assemblages (see text). bdl = below detection limit.

meteorite	chondrule #	mineral	$d^{18}O$	2s	$d^{17}O$	2s	$D^{17}O$	2s
Kaba	Ch-3 (POP)	magnetite	-3.5	1.0	-4.8	0.7	-3.0	1.6
			-4.1	1.0	-5.8	0.7	-3.7	1.6
			-3.7	1.0	-5.1	0.7	-3.2	1.7
			-5.0	1.0	-6.0	0.7	-3.4	1.4
			-3.8	1.0	-5.0	0.6	-3.0	1.6
			-2.4	1.0	-4.1	0.7	-2.8	1.6
			-2.0	1.0	-3.6	0.7	-2.6	1.4
		ol	-5.2	0.9	-8.2	1.2	-5.5	1.7
			-4.7	0.9	-7.9	1.2	-5.4	1.7
			-5.0	1.0	-8.0	1.2	-5.4	1.8
Kaba	Ch-7 (POP)	magnetite	0.1	1.0	-2.0	0.7	-2.0	1.4
			-0.2	1.0	-1.8	0.7	-1.7	1.6
			-0.5	1.0	-1.5	0.7	-1.3	1.6
			0.2	1.0	-1.9	0.7	-2.0	1.6
			-1.5	1.0	-2.7	0.7	-1.9	1.5
			0.5	1.0	-1.3	0.7	-1.6	1.5
		ol	-2.2	0.9	-6.0	1.3	-4.9	1.8
			-1.8	0.9	-6.1	1.3	-5.1	2.0
			-2.6	0.9	-6.7	1.2	-5.4	1.8
Kaba	Ch-12 (POP)	magnetite	-3.3	1.0	-4.5	0.7	-2.8	1.5
			-3.3	1.0	-5.0	0.7	-3.3	1.5
			-2.8	1.0	-4.2	0.7	-2.7	1.5
			-4.0	1.0	-5.3	0.7	-3.2	1.6
			-3.1	1.0	-4.4	0.7	-2.8	1.5
		olivine	-3.5	0.9	-7.1	1.2	-5.3	1.9
			-3.1	0.9	-7.0	1.3	-5.4	1.9
			-3.1	1.0	-7.4	1.2	-5.7	1.7
			-3.5	0.9	-7.2	1.3	-5.4	1.7
Vigarano	Ch-52 (PP)	magnetite	1.2	0.6	-0.4	0.7	-1.0	1.3
			1.1	0.6	-0.3	0.7	-0.9	1.3
			3.3	0.6	1.1	0.6	-0.6	1.3
			3.2	0.6	1.8	0.6	0.1	1.3
			2.1	0.5	0.5	0.6	-0.6	1.3
			2.5	0.6	0.2	0.6	-1.1	1.3
		ol	-2.8	0.9	-6.6	0.9	-5.2	2.0
			-3.0	0.9	-7.0	0.9	-5.4	2.1

table S2. Oxygen isotopic composition of magnetite grains observed in SAM and olivines within chondrules of the Kaba and Vigarano CV3 chondrites. The 2σ errors are obtained by propagation of the errors on the oxygen isotopic composition of standards and the counting statistical error of each measurement of the samples.

meteorite	chondrule #	$d^{34}S$	2s	$d^{33}S$	2s	$D^{33}S$	2s
Kaba	Ch-3	0.3	0.3	0.4	0.2	-0.4	0.5
		0.1	0.3	0.1	0.2	-0.1	0.5
		0.0	0.3	0.0	0.2	0.0	0.5
		0.6	0.3	0.3	0.2	0.0	0.5
		1.0	0.3	0.6	0.2	-0.2	0.5
		0.6	0.3	0.7	0.2	-0.8	0.5
		1.1	0.4	0.8	0.2	-0.5	0.5
		0.9	0.4	0.3	0.2	0.4	0.5
		0.7	0.4	0.1	0.2	0.4	0.5
		0.9	0.4	0.6	0.2	-0.2	0.5
		-0.5	0.4	-0.4	0.2	0.3	0.5
Kaba	Ch-7	1.2	0.4	0.5	0.2	0.3	0.5
		1.0	0.4	0.7	0.2	-0.3	0.5
		1.4	0.3	0.7	0.2	0.1	0.5
		0.2	0.4	-0.1	0.2	0.3	0.6
		0.1	0.4	-0.1	0.2	0.3	0.6
		-0.3	0.3	-0.1	0.2	-0.2	0.5
		0.4	0.4	0.0	0.2	0.3	0.5
		0.6	0.4	0.3	0.2	0.0	0.6
		0.4	0.4	0.2	0.2	-0.1	0.6
		-0.7	0.4	-0.3	0.2	-0.1	0.5
		0.8	0.4	0.2	0.2	0.4	0.6
		-0.3	0.4	-0.2	0.2	0.1	0.6
		0.4	0.4	0.0	0.2	0.4	0.6
		-0.4	0.4	-0.3	0.2	0.1	0.6
		0.4	0.4	0.4	0.2	-0.4	0.6
		0.7	0.3	0.5	0.2	-0.2	0.5
		-0.2	0.3	0.0	0.2	-0.1	0.5
		0.0	0.4	-0.1	0.2	0.1	0.6
		-0.5	0.4	-0.3	0.2	0.1	0.6
		1.0	0.4	0.6	0.2	-0.1	0.6
		0.7	0.4	0.5	0.2	-0.2	0.6
		1.0	0.4	0.6	0.2	-0.1	0.5
		1.0	0.4	0.4	0.2	0.3	0.5
		-0.4	0.3	-0.3	0.2	0.2	0.5
		0.9	0.4	0.5	0.3	-0.1	0.6
		0.4	0.4	0.2	0.2	0.0	0.6
		1.0	0.4	0.6	0.2	-0.1	0.6
Kaba	Ch-12	0.2	0.3	0.2	0.2	-0.1	0.5
		0.5	0.4	0.1	0.2	0.2	0.6
		-0.6	0.4	-0.3	0.2	0.0	0.6
Vigarano	Ch-52	-0.9	0.4	-0.6	0.2	0.2	0.5
		-0.6	0.4	-0.4	0.2	0.2	0.5
		-0.1	0.3	-0.2	0.2	0.3	0.5
		-0.9	0.4	-0.5	0.2	0.1	0.5
		-0.9	0.3	-0.4	0.2	-0.1	0.5
		0.2	0.3	0.0	0.2	0.3	0.5
		-1.0	0.4	-0.6	0.2	0.2	0.5
		-0.2	0.4	-0.1	0.2	0.0	0.5

table S3. Sulfur isotopic composition of sulfide grains observed in FeS-Fe_3O_4 associations within chondrules of the Kaba and Vigarano CV3 chondrites. The 2σ errors are obtained by propagation of the errors on the sulfur isotopic composition of standards and the counting statistical error of each measurement of the samples.